Spectral Analysis of Photoemissive Yields in Si, Ge, GaAs, GaSb, InAs, and InSb

M. L. COHEN* AND J. C. PHILLIPS†
Bell Telephone Laboratories, Murray Hill, New Jersey
(Received 5 March 1965)

The data of Allen and Gobeli on photoemissive yields from partially cesiated surfaces of several semiconductors with photon energies between 2 and 6 eV are analyzed in detail. The results are shown to be consistent with direct transitions in energy-band models obtained from semiempirical pseudopotentials based on interband optical edges. The correlation with reflectivity structure is good, and several new transitions are resolved which were not apparent in previous optical studies.

1. INTRODUCTION

PHOTOEMISSION studies of electrons emitted from atomically clean semiconductor surfaces have yielded information on the electronic structure of Si and several III-V semiconductors about 5 eV above the valence-band edge.[1] The shape of the thresholds is determined by escape mechanisms which involve phase-space factors and electron-phonon interactions.[2]

The purpose of this paper is to discuss the yield curves of cesiated Ge and several III-V semiconductors, specifically, GaAs, GaSb, InAs, and InSb, well above threshold for photon energies between 2 and 6 eV. By covering the surface with a fraction of a monolayer of Cs one can reduce the work function by up to several eV compared to its value for the atomically clean surface. In this way electrons from a larger fraction of the conduction-band states can be studied. Some of the structures associated with band edges in this region have been identified tentatively by optical studies[3] which measure $E_{kc}-E_{kv}$, where $\mathbf{k}$ labels a Bloch state in conduction or valence bands, respectively. The present experiment often gives information on E_{kc} alone, thereby determining absolute rather than relative energies.

Photoemission experiments provide a wealth of information on band structure and escape mechanisms. From very detailed studies of yields and energy distributions in Si it has been concluded[4] that, for a given cesiated surface, $Y(\omega)$—the electron yield per absorbed photon—can usually be interpreted mainly in terms of band structure, assuming constant probability for escape of electrons above vacuum level, and zero probability for escape of electrons below it.[5] For a given surface and fixed photon frequency ω, we can also measure the energy distributions dN/dE of the emitted electrons. While these distributions evidently contain much more information than the yield, it appears at present that they are also much more sensitive to the detailed energy dependence of the escape probabilities.[6] The latter is an involved problem even for Si, so that here we shall be concerned only with the qualitative structure of the yield curves with cesium coverage as a parameter.

We discuss in Sec. 2 the yield curves for Si and Ge using pseudopotential band models based on optical data. A number of features in the yield are correlated with direct-transition edges, which provide detailed confirmation of the optical assignments. In Sec. 3 the detailed analysis is extended by analogy to GaAs, GaSb, InAs, and InSb. Finally, we summarize information gained from the photoemissive yields and compare the results with those of reflectivity studies in Sec. 4.

The experimental yield curves discussed in this paper have been made available to us by Dr. G. W. Gobeli and Dr. F. G. Allen, who will publish more complete results later. The surfaces were produced by cleavage in ultrahigh vacuum,[7] and are the (111) face for Si and Ge and the (110) face for the III-V crystals.[8] Cs was applied by an atomic beam technique[9] and the work function ϕ, defined as the energy difference from the vacuum level to the Fermi level, was measured by the Kelvin method.

To find the vacuum-level position relative to the valence-band maximum one must add to the work function ϕ the separation between Fermi level and valence-band maximum at the surface. This is normally a few tenths of an eV for the clean surface[8] and increases to equal the energy gap E_g for the Cs-covered case since the surface is then strongly n type. The present crystals were of sufficiently high resistivity that band bending was small over the escape depth. This means that for almost all emitted electrons one can place vacuum level $\phi+E_g$ above the valence-band maximum in an $E(\mathbf{k})$ plot.

---

* Present address: Department of Physics, University of California, Berkeley, California.
† Permanent address: Department of Physics, University of Chicago, Chicago, Illinois.

[1] G. W. Gobeli and F. G. Allen, Phys. Rev. **127**, 141 (1962).
[2] E. O. Kane, Phys. Rev. **127**, 131 (1962).
[3] For a recent summary of reflectivity structure in diamond and zincblende-type crystals, see J. C. Phillips, Phys. Rev. **133**, A452 (1964), and Solid State Physics, edited by F. Seitz and D. Turnbull, Vol. 18, (to be published).
[4] F. G. Allen and G. W. Gobeli (to be published).
[5] D. Brust, M. L. Cohen, and J. C. Phillips, Phys. Rev. Letters **9**, 389 (1962). See also, W. E. Spicer and R. E. Simon, Phys. Rev. Letters **9**, 387 (1962), and D. Brust (to be published).
[6] E. O. Kane (private communication).
[7] G. W. Gobeli and F. G. Allen, J. Phys. Chem. Solids **14**, 23 (1960).
[8] G. W. Gobeli and F. G. Allen, Phys. Rev. **137**, A245 (1965).
[9] F. G. Allen and G. W. Gobeli, Rev. Sci. Instr. **34**, 184 (1963).

2. YIELD SPECTRA OF Si AND Ge

Before proceeding to a detailed analysis of Ge, we wish to review the logical content of our combined theoretical and experimental approach. Our aim is to show that while the assignments of optical edges were plausible and consistent with band models,[1] when these are combined with the present photoemission data the final models are unambiguous, with a resolution in energy $\Delta E<0.2$ eV, and a resolution in the Brillouin zone $\Delta k<0.2K_{BZ}$, where K_{BZ} is a Brillouin-zone diameter.

We may divide the bands to be studied into valence and conduction bands. All calculations of the valence bands of diamond-(zincblende)-type crystals have yielded qualitatively similar results. The highest level is $\Gamma_{25'}(\Gamma_{15})$, then $L_{3'}(L_3)$, then $X_4(X_5)$, and finally $W_2(W_3,W_4)$. The width of these bands decreases as we go from less ionic to more ionic crystals, but the general shape is always the same.

The situation is much more complex in the conduction bands. Several of the conduction bands ($\Gamma_{2'}$ and L_1 in diamond crystals) are extremely sensitive to small changes in crystal potential.[3] The position of these edges (and also X_1, Γ_{15}, and L_3) must be established experimentally. After this has been done, however, we find that the general shape or topology of the bands between symmetry points is determined by the nearly free-electron or pseudopotential model. Although the pseudopotential models[3] constructed for Si and Ge contain three parameters each, the fit to experiment is so complete as to leave no doubt as to the correctness of the band shapes derived. In the case of Si, for instance, three parameters fit 20 energy gaps and effective masses with errors of less than 20%.

The most conclusive assignment of interband structure to a certain region of the Brillouin zone is obtained through spin-orbit splittings. These establish the correctness of $L_{3'}\rightarrow L_1$ and $L_{3'}\rightarrow L_3$ assignments.[3] Recently the spin-orbit splitting of X_5 (which is zero in diamond crystals and small in zincblende crystals) has been resolved[10] in HgSe and HgTe in the peak previously assigned to $X_5\rightarrow X_1$ transitions.[5] However, the photoemission data discussed earlier[5] for Si (as well as the data discussed here for Ge and the III-V's)also demonstrate the correctness of this assignment, as we shall see.

The greatest ambiguities arise near points of degeneracy. The most difficult case is $\Gamma_{25'}\rightarrow\Gamma_{15}$. Neglecting spin the levels are both threefold degenerate. Whereas the topology of interband energy surfaces near $\Gamma_{25'}\rightarrow\Gamma_1$ is unambiguous, the highest $\Gamma_{25'}$ band $\rightarrow$ lowest Γ_{15} band surfaces may be extremely complex, depending on six effective mass parameters (three each for $\Gamma_{25'}$ and Γ_{15}).

For other edges it is sufficient to identify critical points, defined by

$$\nabla_k(E_{kc}-E_{kv})=0 \qquad (2.1)$$

at or near symmetry points. These establish the line shape of the optical structure and mark the energies at which the structure occurs. The resolution in k space is usually better than $0.1K_{BZ}$, and in energy is limited only by lifetime broadening and unresolved (or partially resolved) excitons, which give $\Delta E<0.1$ eV.

In these respects $\Gamma_{25'}\rightarrow\Gamma_{15}$ is our worst case. The effective masses of the split-off $J=\frac{1}{2}$ bands are so small that no spin-orbit splitting is resolved in the optical spectra. Moreover, because of the high degree of degeneracy, the interband surfaces near $\Gamma_{25'}\rightarrow\Gamma_{15}$ tend to contain clusters of critical points,[3] e.g., one at Γ, and one or two groups along the [100] and [110] axes, 0.1 or 0.2 K_{BZ} away from Γ. The internal structure of these clusters is so sensitive to the six effective-mass parameters as to make it impossible to specify from the present data which is responsible for the observed structure, which is spread over 0.2 eV. On the other hand, because $\Gamma_{25'}$ is the top of the valence band, we will show beyond doubt that certain structure in the optical spectra and photoemissive yields comes from the clusters of critical points contained in a region of k space within 0.2 K_{BZ} of $\Gamma_{25'}\rightarrow\Gamma_{15}$. As an example we review the results[5] for Si, Fig. 1. The experimental yield rises steeply near 3.4 eV because of the onset of direct transitions from the region near $\Gamma_{25'}$ to states

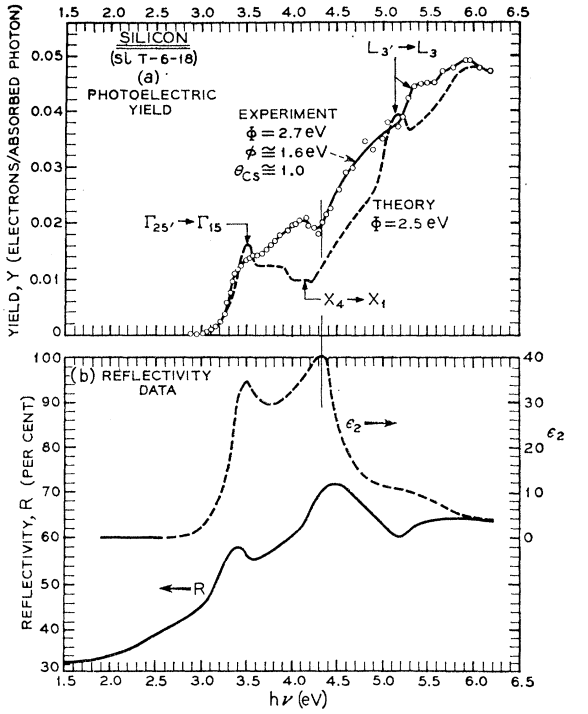

FIG. 1. (a) Photoelectric yield from Cs-covered silicon. Experimental results of Allen and Gobeli (Ref. 4) compared with theory of Brust, Cohen, and Phillips (Ref. 5). (b) Reflectivity data of Philipp and Ehrenreich (Ref. 14).

[10] W. J. Scouler and G. B. Wright, Phys. Rev. **133**, A736 (1964).

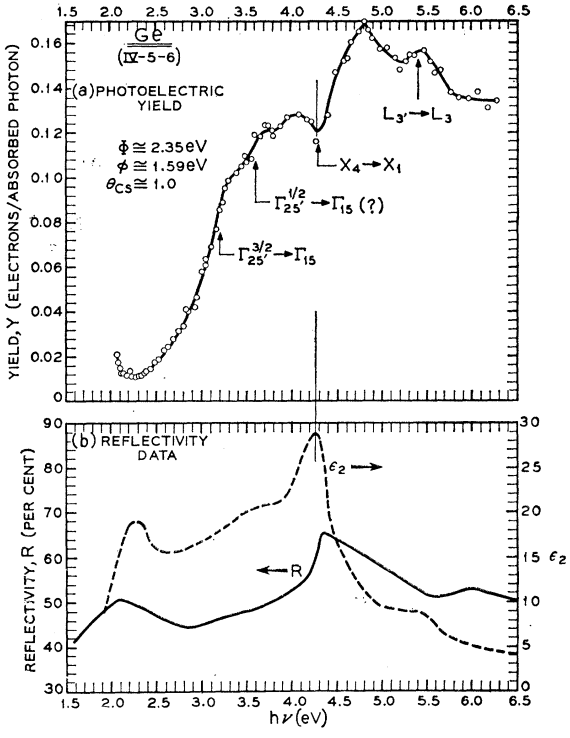

FIG. 2. (a) Photoelectric yield from Cs-covered germanium (Allen and Gobeli, Ref. 4). (b) Reflectivity data of Philipp and Taft.

near Γ_{15} above vacuum level. The theoretical yield rises steeply at nearly the same energy because the pseudopotential[5] was adjusted to make $\Gamma_{25'} \rightarrow \Gamma_{15}$ fit an optical energy gap of 3.5 eV. Note that the width of this peak is 0.4–0.5 eV.

The next striking feature of the Si data is the narrow dip near 4.3 eV, which correlates well with a reflectivity peak at 4.5 eV and an ϵ_2 peak at 4.3 eV assigned to $X_4 \rightarrow X_1$. The width of the dip is 0.2 eV. The final states near X_1 are well below vacuum level, so that transitions to the neighborhood of X_1 would be expected to cause a dip in yield.

Although no optical structure is found between 4.5 and 5.0 eV, theory[5] and experiment[8] agree in predicting a rapidly rising yield. This may be ascribed to the average effect of energy surfaces throughout the Brillouin zone rather than the contribution of a particular region of the zone.

The last clearly resolved optical structure is a weak peak in the reflectivity near 5.5 eV and in ϵ_2 near 5.3 eV. A steep rise in yield is found with shoulder at 5.3 eV. This is ascribed to $L_{3'} \rightarrow L_3$ transitions with L_3 well above vacuum level.

Although the over-all agreement with experiment of the calculated yield curves for a wide range of Cs coverages is impressive for Si, one may inquire whether the line shapes observed are truly characteristic of the bulk energy bands. The over-all similarity of line shape of optical spectra of Si, Ge, and many III-V and II-VI zincblende crystals[3] suggests that this is the case. Such similarity also holds for the yield curves of Si, Ge, GaAs, GaSb, InAs, and InSb, as seen from Figs. 1, 2, 4, 6, 8, 10, 11, and 12. The peak $\Gamma_{25'} \rightarrow \Gamma_{15}$ is always present and usually well resolved, and the $X_4 \rightarrow X_1$ dip is always easily identified. Such obvious features of the yield invite us to examine the data for further structure.

Consider the yield curves for Ge shown in Fig. 2. In the energy range $3.0 \leq \hbar\omega \leq 4.0$ eV where the yield rises rapidly, a strong shoulder is present at 3.25 ± 0.05 eV and a weaker shoulder at 3.5–3.6 eV. Structure near 3.2 eV in the optical spectrum of Ge has been assigned[3] to $\Gamma_{25'} \rightarrow \Gamma_{15}$ transitions. By analogy with Si we identify the strong shoulder with $\Gamma_{25'}{}^{3/2} \rightarrow \Gamma_{15}$ and the weak shoulder with the split-off valence band, $\Gamma_{25'}{}^{1/2} \rightarrow \Gamma_{15}$, which has not been identified positively in the optical spectrum. The separation of the shoulders is compatible with the spin-orbit splitting of $\Gamma_{25'}$, which is 0.29 eV, according to infrared studies of free-carrier absorption.[11] It is interesting that the weak shoulder associated with the split-off band is not resolved in the optical spectrum because of the large background associated with other regions of the zone.

The familiar dip at 4.3 eV coincides, as in Si, with the $X_4 \rightarrow X_1$ peak in the optical spectrum. Also a strong $L_{3'} \rightarrow L_3$ peak is found at 5.4 eV. It appears that either the oscillator strength of this transition is significantly greater in the group-IV crystals, or the lifetime of L_3 is longer, compared to the III-V crystals, because the $L_{3'} \rightarrow L_3$ peaks are significantly stronger in the Si and Ge yield spectra.

It is interesting to note that from Allen and Gobeli's complete data the $\Gamma_{25'} \rightarrow \Gamma_{15}$ shoulders disappear with increasing work function only when vacuum level is 3.4 eV above the top of the valence band. This means that the transitions contributing to the sharp rise in yield at 3.2 eV must start within 0.4 eV of the top of the valence band. More narrow limits ($\leq$0.2–0.3 eV) for the transitions are established by the more complete data on Si[4] and GaAs.

At this point we wish to remark on the correlation between edges in the optical reflectivity and photoemissive yield. The fundamental optical parameter, which is proportional to the joint interband density of states, is $\epsilon_2 = 2nk$. Structure in the reflectivity

$$R = \frac{(n-1)^2 + k^2}{(n+1)^2 + k^2}$$

has been found to correlate quite well with similar structure in ϵ_2. However, near strong peaks in R or ϵ_2 one finds that there is usually some dispersion in the edge energies of R, n, k, and ϵ_2. The largest dispersion for zincblende crystals is associated with the $X_5 \rightarrow X_1$ peak. Two examples obtained by Kramers-Kronig

[11] R. Braunstein and E. O. Kane, J. Phys. Chem. Solids 23, 1423 (1962).

TABLE I. Energies (in eV) of optical parameters for $X_5 \rightarrow X_1$ edges, according to M. Cardona (private communication).

	T(°K)	R	k	n	ϵ_2
InP	300	5.00	4.96	4.62	4.77
ZnTe	77	5.44	5.38	4.74	5.06

transforms of reflectance data are shown in Table I; the dispersion for InP is typical of III-V crystals, while that of ZnTe represents an extreme case.[12] Note that the edge in R falls close to the edge in k, but that the edge energy in ϵ_2 represents the harmonic mean between the edge energies in n and k. We have allowed for this correction in our analysis, which quotes optical edges in ϵ_2.

We should also note that systematic sampling of the Brillouin zone[5] also predicts that dips or peaks in yield in reflectivity will be located 0.1 or 0.2 eV away from the interband energy differences just at a symmetry point. With extensive band calculations[5] throughout the zone available to guide us, we have been able to correct for this shift in comparing yield structure with edges in ϵ_2. In conclusion we note that corrections of both kinds are expected to be small (<0.1 eV) for $\Gamma_{15v} \rightarrow \Gamma_{15c}$, which accounts for the excellent agreement obtained with regard to the 3.5-eV edge. For the $X_5 \rightarrow X_1$ peak the corrections are larger and are included specifically.

3. ELECTRONIC STRUCTURE OF GaAs, GaSb, InAs, InSb

In previous work the vacuum level of (110) atomically clean GaAs surfaces has been placed 4.66 eV above the conduction-band edge Γ_{1c} in the bulk.[8] Allen and Gobeli have shown that, again relative to the bulk, the vacuum level can be lowered to only 1.49 eV above Γ_{1c} by covering the surface with one monolayer of Cs. Referring to the energy bands[13] of GaAs shown in Fig. 3, we see that for zero cesium coverage the vacuum level passes about 0.5 eV above L_{3c} and 1.8 eV above Γ_{15c}.

As cesium coverage is increased, the vacuum level decreases through Γ_{15c} and a rise in yield associated

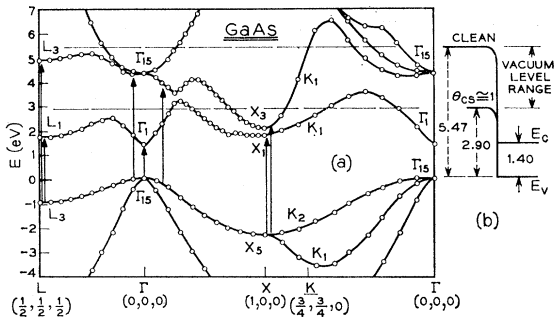

FIG. 3. (a) Energy-band diagram of GaAs calculated by the pseudopotential method (M. L. Cohen, Ref. 13). (b) Energy levels at the clean and cesium-covered (110) surfaces (Gobeli and Allen, Ref. 8).

with the onset of transitions at or near $\Gamma_{15v} \rightarrow \Gamma_{15c}$ is expected for a certain minimum photon energy $\hbar\omega_0$. Referring to Fig. 4, we see that the yield begins to rise sharply near $A_1 = \hbar\omega_0 = 4.50$ eV for vacuum level 3.15 ± 0.3 eV above the conduction-band edge Γ_{1c}. With $\Gamma_{1c} - \Gamma_{15v}^{3/2} = 1.35$ eV, we see that the vacuum level is just passing through Γ_{15c} which is about 4.50 eV above $\Gamma_{15v}^{3/2}$. In this way we confirm the identification of the A_1 edge in the optical reflectivity at 4.52 eV as derived from the contribution of the $\Gamma_{15v} \rightarrow \Gamma_{15c}$ region to the band-4–band-6 joint density of states, and place the initial and final states absolutely in energy. In particular, the initial states must be within 0.3 eV of the valence-band maximum. According to Fig. 3(a) this confines us closely to the neighborhood of $\Gamma_{15v}^{3/2}$.

The next prominent feature is the dip in yield near 5.0 eV which is marked B in Fig. 4. For the curves with smaller yield when the vacuum level is 2.0 eV or more above Γ_{1c} it is not clear whether we are dealing with a dip, or whether we should regard peak A as superimposed on a smoothly varying background, with peak A beginning to fade out near 4.7 eV up to 5.0 eV. However, the last three larger yield curves, with vacuum level from 1.5 to 2.1 eV above Γ_{1c}, definitely show a dip below background centered near 4.95 eV. A dip of this kind was found previously in Si, and it was shown by direct calculation[5] based on a Si pseudopotential band structure to be associated with the $X_4 \rightarrow X_1$ and $K_3 \rightarrow K_1$ interband edges which produce the largest peak in ϵ_2. The $X_5 \rightarrow X_1$ peak in the reflectivity of GaAs occurs at 5.12 eV. However, before identifying dip B with the $X_5 \rightarrow X_1$ edge, we discuss the corrections which must be made to reflectivity and photoemission data to obtain the true $X_5 \rightarrow X_1$ energy associated with the interband edge in ϵ_2.

Kramers-Kronig transforms[14] of room-temperature reflectivity data place $X_5 \rightarrow X_1$ at 4.65 eV for ϵ_2. This is rather lower than the position of dip B in the yield. However, yield curves for Si, derived from a pseudo-

[12] M. Cardona (private communication).

[13] The energy bands shown in Fig. 3 were obtained at the points indicated by one of us (MLC) using a pseudopotential constructed to fit interband optical energy differences in a manner similar to that of Ref. 5. To allow for the presence of two different atoms in the unit cell, the pseudopotential for GaAs was divided into a symmetric part V_S and an antisymmetric part V_A. The parameters used for V_S were the ones that give a best fit to the Ge band structure. On the other hand, V_A is found to be small and is determined in first approximation by a point ion approximation. (The actual values of the V_A parameters were of course determined by fitting the optical spectrum of GaAs.) For our present purposes it is sufficient that the energy bands of Fig. 3 are consistent with the optical spectra at interband critical points and give an accurate interpolation throughout the Brillouin zone. A complete account of these calculations will be given elsewhere (M. L. Cohen, to be published).

[14] H. R. Philipp and H. Ehrenreich, Phys. Rev. **129**, 1550 (1963).

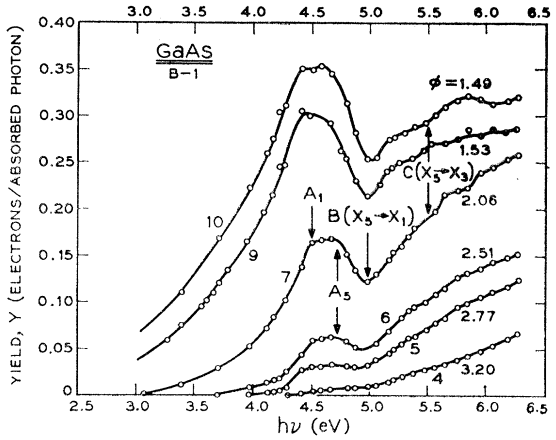

FIG. 4. Photoelectric yield of GaAs at various Cs coverages (Gobeli and Allen).

potential band structure,[5] show that the $X_4 \rightarrow X_1$ dip first becomes pronounced with vacuum 2.5 eV above X_1. At this vacuum level although $X_4 \rightarrow X_1$ occurs at 4.0 eV, the center of the dip is at 4.2 eV. As the vacuum is lowered to 1.5 eV above X_1 the dip shifts to 4.3 eV. It is finally centered at 4.0 eV when the vacuum level is only 0.5 eV above X_1.

In GaAs X_{1c} is believed[15] to be 0.35 eV above Γ_{1c}. Thus for the yield curves for which the dip is most prominent the vacuum is 1.05 to 1.35 eV above X_{1c}; the Si theoretical yield curves lead us to expect that the dip will be located 0.3 eV above the ϵ_2 energy of 4.65 eV. This value of 4.95 eV agrees quantitatively with the observed value. Moreover, the shift in the dip from 4.9 eV above X_{1c} is just what would be expected from the Si theoretical yield curves.[5]

A characteristic feature of zincblende semiconductors is the splitting of the twofold degenerate conduction-band level X_{1c} in diamond crystals into $X_{1c}+X_{3c}$. Interband edges associated with $X_{5v} \rightarrow X_{1c}$, X_{3c} have been resolved at low temperatures in GaAs, GaSb, InAs, and InSb.[16] The $X_5 \rightarrow X_{3c}$ edge is much weaker than $X_5 \rightarrow X_{1c}$, as one would expect from the $E(\mathbf{k})$ curves shown in Fig. 3. (Both the longitudinal and transverse masses near X_{1c} are much larger than those near X_{3c}.) In fact, at room temperature the $X_5 \rightarrow X_{3c}$ edge is resolved only in InAs. At first one would not expect to detect $X_5 \rightarrow X_{3c}$ structure in the photoemissive yields, which is broadened more by electron-phonon interaction than the room-temperature reflectivity (see below for a discussion of line shapes). However, one must bear in mind that a low vacuum level just above X_{1c} and X_{3c} tends to enhance the importance of these levels. Together with somewhat smaller regions of k space near Γ and L, the neighborhoods of X_{1c} and X_{3c} are then the only regions from which photoelectrons will not be emitted.

The optical value for the $X_{3c}-X_{1c}$ splitting is 0.43 eV in GaAs.[16] In the three largest yield curves (vacuum level 0.65 and 0.89 eV above X_{3c}) a weak dip labeled C is observed between 5.5 and 5.6 eV. The center of this dip agrees, within the spacing of the experimental points, with the position expected from optical data (4.95+0.43 eV). The dip persists to the next two yield curves (vacuum up to 1.7 eV above X_{3c}).

Line shape. A quantitative discussion of line shape requires surveying the pseudoptotential energy bands throughout 50 000 points in the zone to obtain yield curves,[5] and about 500 000 points to obtain energy distributions (resolution 0.1 eV). We have not carried out such a survey, but we wish to comment qualitatively on the resolution of the structure marked A_1 and A_5 in the yield curves (Fig. 4).

When the absorption length is small compared to the mean free path for an electron to emit or absorb phonons, the bulk of the photoemitted electrons will have escaped without inelastic scattering. In this case, assuming uniform cesium coverage and neglecting the effects of band bending near the surface, we expect the thermal broadening of the yield spectrum to be very close to that of the reflectivity.

With no inelastic scattering we find from studying 4–6 energy contours[13] near Γ that structure may arise from a cluster of critical points in this region. For the energy bands of GaAs shown in Fig. 3, the cluster consists of

$$M_0 \text{ at } \mathbf{k}_0=(0.25,0,0) \text{ and } 4.08 \text{ eV},$$
$$M_1 \text{ at } k_1=(0.2,0.2,2,0) \text{ and } 4.21 \text{ eV},$$

and a degenerate saddle-point edge of general type M_2 at Γ with the $\Gamma_{15v}-\Gamma_{15c}$ energy difference of 4.36 eV.

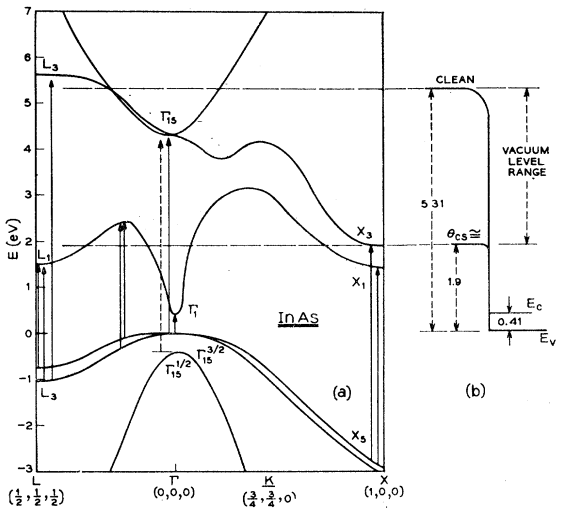

FIG. 5. (a) Energy-band diagram of InAs, sketched free-hand from optical data (Ref. 16) and by analogy with Fig. 3. (b) Energy levels at the clean and cesium-covered surfaces (Gobeli and Allen, Ref. 8).

[15] O. G. Folberth and H. Weiss, Z. Naturforsch **10A**, 615 (1955).
[16] D. L. Greenaway and M. Cardona, *Proceedings of the International Conference on the Physics of Semiconductors, Exeter* (The Institute of Physics and the Physical Society, London, 1962), p. 666.

Of course, the structure of this cluster is rather dependent on the details of the energy-band model. Nevertheless, the range in energy of the critical points is about 0.3 eV, which agrees qualitatively with the difference of 0.25 eV between A_1 and the second edge marked A_5 in Fig. 4. Within the framework of the energy-band model shown in Fig. 3, $\Gamma_{15c} \rightarrow \Gamma_{15v}$ is more likely to be assigned to A_5 than to A_1. The cluster of critical points is spaced so close to Γ, however, as to make it difficult to establish this point with certainty even with the aid of energy distributions.

The broad tail in the yield for $\hbar\omega < 4.5$ eV has the shape that one would obtain from a step function, centered at 4.5 eV, which has undergone phonon-induced broadening. The half-width of this broadening, which is superposed on a background of $4 \rightarrow 5$ transitions, seems to be less than 0.2 eV.

InAs. Apart from the direct gap, which is at 1.35 eV in GaAs and 0.4 in InAs, the optical edges in InAs fall at the same energies as those of GaAs (within 0.2 eV). For this reason we may assume that the valence-band structure of InAs is the same as GaAs, and use interband-edge energies in $\epsilon_2(\omega)$ as inferred from reflectivity and Kramers-Kronig transforms to sketch the energy bands of InAs [see Fig. 5(a)]. In particular we assume that the energy difference $\Gamma_{15v} - X_{5v}$ is the same in the two crystals. Because $X_{1c} - \Gamma_{15v}$ is known in GaAs, this enables us to place X_{1c} above Γ_{15v} in InAs by 1.40 eV. The range of the vacuum level with $\theta = 0$ monolayers of Cs to $\theta = 1$ is indicated in Fig. 5(b).

The yield curves for a range of Cs coverages are shown in Fig. 6. The most prominent features of the curves are the doublet peaks at 4.3 and 4.7 eV. These are assigned to transitions near $\Gamma_{15v}^{3/2} \rightarrow \Gamma_{15c}$ and $\Gamma_{15v}^{1/2} \rightarrow \Gamma_{15c}$. The best value[11] for the $\Gamma_{15v}^{3/2}$–$\Gamma_{15v}^{1/2}$ splitting is 0.43 eV, which agrees well with the separation of the peaks. The relative strengths of the peaks are difficult to determine because of unknown background contributions.

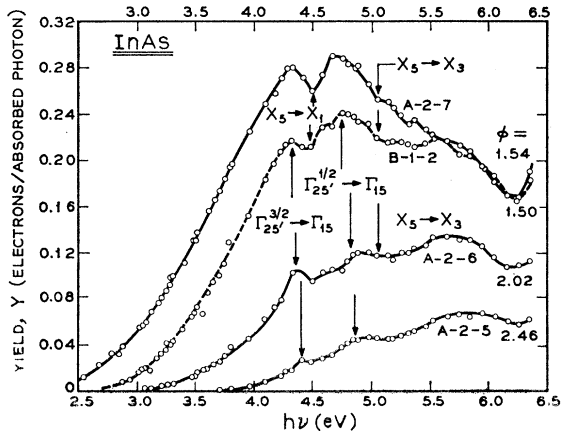

FIG. 6. Photoelectric yield of InAs at various Cs coverages (Gobeli and Allen, Ref. 8).

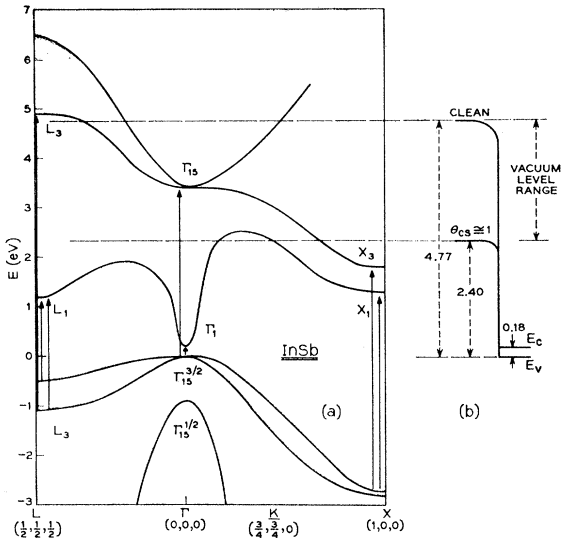

FIG. 7. (a) Energy-band diagram for InSb, sketched free-hand from optical data (Ref. 16) and by analogy with Fig. 3. (b) Energy levels at the clean and cesium-covered surfaces (Gobeli and Allen, Ref. 8).

Again we can place lower limits on the energy of the final states responsible for these peaks. The complete data of Gobeli and Allen show that the peaks are present in the yield curve with vacuum level 3.6 eV above Γ_{15v}. They are absent when the vacuum lies above Γ_{15c}. This was to be expected, because the cluster of critical points near Γ mentioned in the preceding section is concerned with Δ_1 and Σ_1 final states below Γ_{15c}, which itself is 4.3 eV above $\Gamma_{15v}^{3/2}$.

We now turn our attention to the $X_5 \rightarrow X_1$ and $X_5 \rightarrow X_3$ dips which, according to reflectivity data, are separated by 0.47 eV. The $X_5 \rightarrow X_1$ dip falls at 5.0 eV in GaAs, while the $X_5 \rightarrow X_1$ optical peak of InAs is 0.3 eV lower than the corresponding peak in GaAs. Thus we expect a strong dip at about 4.7 eV in InAs associated with $X_5 \rightarrow X_1$ and a weak dip at 5.2 eV associated with $X_5 \rightarrow X_3$.

In fact, with the vacuum level 0.7 eV above X_{1c} a broad trough is found between the doublet peaks extending from 4.50 to 4.75 eV. Clearly the line shape of the dip is distorted by the superposed doublet peaks. A weak dip is also seen at 5.05 eV which can be attributed to $X_5 \rightarrow X_3$.

As the vacuum level is lowered ($\theta \rightarrow 1$), the volume of phase space near X_{1c} and X_{3c} where electrons will not escape from the crystal steadily decreases. Thus the dip at 4.5 eV where the vacuum level is practically coincident with X_1 need not necessarily mark the true $X_5 \rightarrow X_1$ energy difference; it may simply reflect the line shape of the $\Gamma_{15v}^{\alpha} \rightarrow \Gamma_{15c}$ ($\alpha = \frac{3}{2}, \frac{1}{2}$) doublet.

We can gain further insight into the strength of dips as the vacuum level approaches a band edge by studying the $X_5 \rightarrow X_3$ dip. As the vacuum level is lowered, the dip weakens and has almost disappeared when the vacuum level is 0.2 eV *below* X_3.

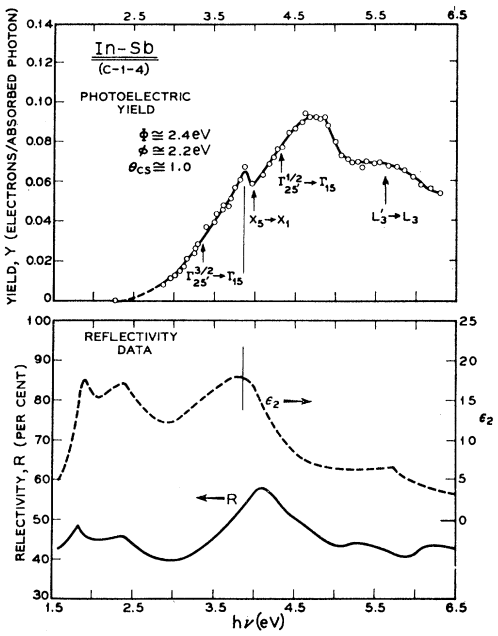

FIG. 8. Above: Photoelectric yield of Cs-covered InSb. Below. Reflectivity data of Philipp and Ehrenreich, Ref. 14.

InSb. Because both atoms belong to the fifth row of the periodic table all interband energies tend to be 10–20% smaller than in GaAs. The energy-band spectrum sketched from optical data is shown in Fig. 7. The most prominent feature of the yield spectrum (Fig. 8) is the dip at 4.0 eV associated with $X_5 \to X_1$. There is some evidence for $\Gamma_{15}^{3/2} \to \Gamma_{15}$ and $\Gamma_{15}^{1/2} \to \Gamma_{15}$ at 3.4 and 4.3 eV, respectively, but the peaks are weak and are superposed on a rapidly rising background, so that the structure is not readily distinguishable from experimental scatter. A broad, weak peak in the yield between 5.3 and 5.9 eV can be assigned to $L_{3v} \to L_{3c}$ transitions, in agreement with spin-orbit split reflectivity peaks which are observed[14] at 5.4 and 6.0 eV.

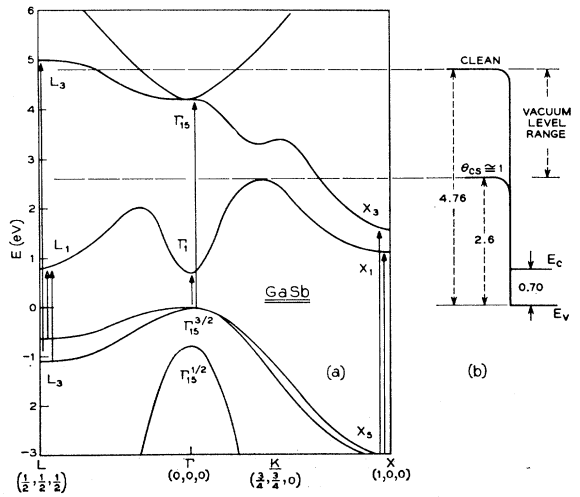

FIG. 9. (a) Energy-band diagram for GaSb, sketched free-hand from optical data (Ref. 16) and by analogy with Fig. 3. (b) Energy levels at the clean and cesium-covered surfaces (Gobeli and Allen, Ref. 8).

GaSb. The band structure is sketched in Fig. 9. The positions of the L_{1c} and X_{1c} edges relative to $\Gamma_{15}^{3/2}$ are known through alloy absorption threshold studies.[17,18] When combined with reflectivity edges these enable us to establish the band structure completely at Γ, L, and X in the energy range of interest. The shape of the bands along [100] and [111] axes is determined by analogy with the GaAs bands.

The yield for Cs-covered GaSb is shown in Fig. 10. The $X_5 \to X_1$ and $X_5 \to X_3$ dips are resolved at 4.17 and 4.5 eV, respectively. The splitting of 0.33 eV agrees qualitatively with the value of 0.47 eV obtained from optical studies.[16] Shoulders which can be assigned to $\Gamma_{15}^{3/2} \to \Gamma_{15}$ and $\Gamma_{15}^{1/2} \to \Gamma_{15}$ are present at 3.7 and 4.4 eV, respectively. The splitting of 0.6 eV agrees qualitatively with the expected splitting of 0.7–0.8 eV. The $L_{3v} \to L_{3c}$ peak expected near 5.7 eV may be present, but experimental scatter is too great to be certain.

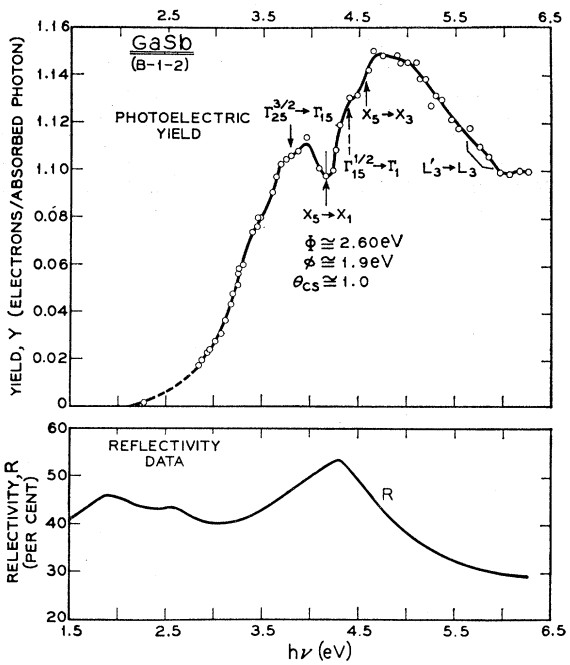

FIG. 10. Above: Photoelectric yield of Cs-covered GaSb, (Gobeli and Allen). Below: Reflectivity data of M. Cardona.

4. CONCLUSIONS

The analysis of the position and width of peaks and dips in yield from semiconductors with partially cesiated surfaces given in the preceding sections has necessarily been detailed and complex. In order to

[17] I. I. Burdiyan, Fiz. Tverd. Tela **1**, 1360 (1959) [English transl.: Soviet Phys.—Solid State **1**, 1246 (1960)].

[18] A. L. Edwards and H. G. Drickamer, Phys. Rev. **122**, 1149 (1961).

TABLE II. Comparison of energies (in eV) for the two most prominent features in the reflectivity and yield spectra of Ge and four III–V semiconductors.

	R(80°K)	Y(300°K)
Dip:		
$X_5 \rightarrow X_1$:		
Ge	4.4	4.3
GaAs	5.12	5.0
InAs	4.83	4.6
InSb	4.20	4.0
GaSb	4.33	4.17
Peak:		
$\Gamma_{25}{}^{3/2} \rightarrow \Gamma_1$:		
Ge	3.2	3.25
GaAs	4.52	4.5–4.7
InAs	4.63	4.36
InSb	3.45	3.4
GaSb	3.74	3.7

extract the maximum information from Gobeli and Allen's data we have been compelled to explore some rather mathematical aspects of energy surfaces in **k** space. We have also found it necessary, in comparing the photoemission data with optical data, to take into account a number of small corrections that vary in magnitude from crystal to crystal.

The results of our efforts for the two principal features of the yield spectrum are summarized for the six crystals in Table II. The over-all agreement between optical and photoemissive data is better than 0.2 eV. We feel that the differences can probably be explained solely in terms of dispersion displacements between ϵ_2 and R, as discussed in connection with Table I. We

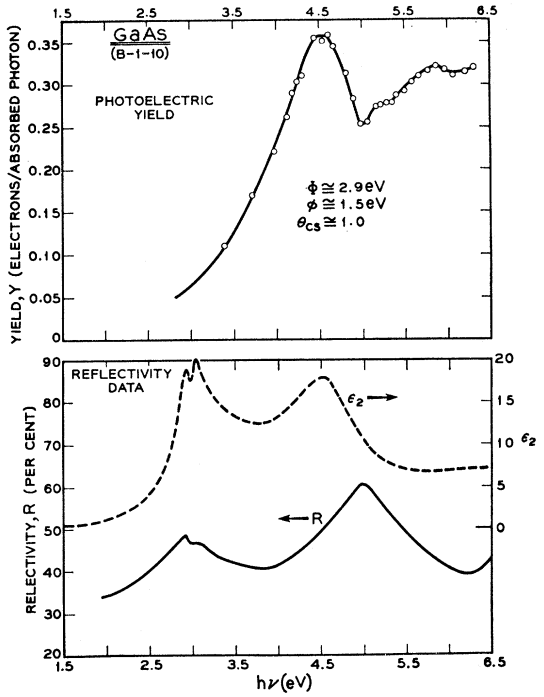

FIG. 11. Above: Photoelectric yield of GaAs (Gobeli and Allen). Below: Reflectivity data of Philipp and Ehrenreich, Ref. 14.

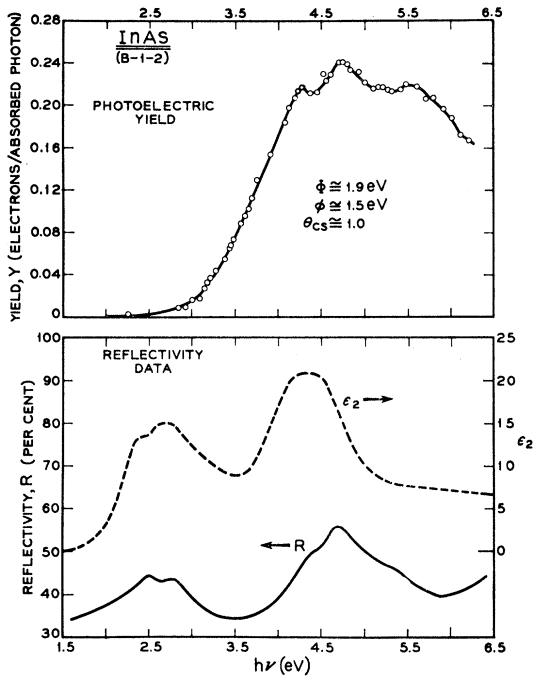

FIG. 12. Above: Photoelectric yield of InAs (Gobeli and Allen). Below: Reflectivity data of Philipp and Ehrenreich, Ref. 14.

believe that the peak values of ϵ_2 derived from Kramers-Kronig transforms given, e.g., in Ref. 14, are unlikely to be accurate to better than 0.2 eV. Thus the over-all correlation is quite satisfactory, as shown in simple form for GaAs in Fig. 11 and for InAs in Fig. 12. We have substantiated this correlation with many additional details in the preceding sections.

Our analysis also establishes the correctness of Allen and Gobeli's data in several larger senses. Detailed examination and comparison of the line shapes shown in Figs. 2, 4, 6, 8, and 10 show that internal scatter and irregularities in the data are generally less than 0.1 eV. This is true for the fully cesiated surface, $\theta \simeq 1$, but it also holds equally well for the partially cesiated surfaces with vacuum level at a value intermediate between that of the clean and fully cesiated surfaces.

We may note that probably most of the optical transitions taking place in these crystals are direct (**k**-conserving). This was to be expected, in view of the large static dielectric constants which reduce electron-electron and electron-phonon interactions. Moreover, below 6 eV the phase space available for Auger excitation of valence electrons is quite small. Because of large dielectric screening the oscillator strength of excitons in this region is expected to be small, and the present data contain no evidence for exciton formation in the fundamental absorption region.

We close by mentioning fine points in the band structure of these crystals which have been observed. These include the resolution at 300°K of the X_{3c}–X_{1c} splitting in the conduction bands of the III-V com-

pounds as well as the placement of X_{3c} relative not only to X_5 but also to Γ_{15v}. Furthermore in most cases the $\Gamma_{15v}{}^{\alpha} \rightarrow \Gamma_{15c}$ ($\alpha = \frac{3}{2}, \frac{1}{2}$) thresholds are separated, which has not proved possible so far in most optical spectra.

ACKNOWLEDGMENTS

The authors wish to express their deep appreciation to F. G. Allen and G. W. Gobeli for permission to analyze and publish some of their very fine experimental data prior to their own more complete publication. We also benefited from conversations with D. Brust, M. Cardona, and E. O. Kane. This work was performed during a summer visit by one of us (JCP) to Bell Laboratories (Murray Hill), and we wish to express to the staff of the laboratories, particularly the theoretical physics group, our gratitude for their kind hospitality.

PHYSICAL REVIEW VOLUME 139, NUMBER 3A 2 AUGUST 1965

Stress Effects on Impurity-Induced Tunneling in Germanium*

H. FRITZSCHE

Department of Physics and Institute for the Study of Metals, The University of Chicago, Chicago, Illinois

AND

J. J. TIEMANN

General Electric Research Laboratory, Schenectady, New York

(Received 10 March 1965)

The effects of uniaxial compression and of hydrostatic pressure on the impurity-induced interband tunneling current in germanium tunnel junctions have been studied experimentally at 4.2°K. The diodes were formed on (100) and (110) faces of arsenic-doped germanium bars. The stress coefficients of the tunnel current were measured at fixed forward and reverse bias voltages. The experiments show that the part of the electron wave function responsible for impurity-induced tunneling is not associated with a particular conduction-band valley. Some structure in the bias dependence of the shear stress coefficients near zero bias remains unexplained. This structure does not appear in the hydrostatic-pressure coefficient.

I. INTRODUCTION

THERE are three distinctly different interband tunneling processes[1–4] in semiconductors: (i) direct tunneling between states having the same value of the crystal momentum k, (ii) phonon-assisted tunneling between states of different k, and (iii) impurity-induced tunneling. This last tunneling process again occurs between states of different k, but in this case the difference in crystal momenta of the initial and final electron states is supplied by impurities or defects.

All three tunneling processes can be observed in Ge or Si tunnel junctions in different bias ranges.[3–5] In Ge, the relative amount of phonon-assisted and impurity-assisted indirect tunneling depends strongly on the donor element.[6,7] The fraction of impurity-induced tunneling increases with increasing magnitude of the central cell potential of the particular donor element. In Sb-doped germanium, impurity-induced tunneling is almost completely negligible with respect to phonon-assisted tunneling, and the reverse is true for As- and P-doped Ge.

Recently[8,9] many details of the direct and the phonon-assisted indirect tunneling processes have been uncovered by measuring the bias dependence of the effect of pressure and shear stress on the tunneling current in Sb-doped germanium tunnel diodes. The absence of impurity-induced tunneling in these samples made it possible to get some clear answers concerning the other processes.

The work discussed here on As-doped tunnel diodes complements the previous work in that the impurity-induced tunneling current in these samples completely dominates the phonon-assisted components.

There are several questions concerning this mode of tunneling that can be answered by stress experiments. In particular, it has been shown[8] that the presence or absence of a large positive shear stress coefficient for current I along [1$\bar{1}$0] and compressional stress along

* The research reported in this paper was sponsored by the Air Force Office of Scientific Research through Grant No. AFOSR 148-63.

[1] L. Esaki, Phys. Rev. **109**, 603 (1958).

[2] E. O. Kane, J. Appl. Phys. **32**, 83 (1961).

[3] H. Holonyak, Jr., I. A. Lesk, R. N. Hall, J. J. Tiemann, and H. Ehrenreich, Phys. Rev. Letters **3**, 167 (1959).

[4] J. V. Morgan and E. O. Kane, Phys. Rev. Letters **3**, 466 (1959).

[5] R. N. Hall and J. H. Racette, J. Appl. Phys. **32**, 2078 (1961).

[6] R. N. Hall, in *Proceedings of the International Conference on Semiconductor Physics, Prague, 1960* (Academic Press Inc., New York, 1961), p. 193.

[7] Y. Furukawa, J. Phys. Soc. Japan **15**, 1903 (1960).

[8] H. Fritzsche and J. J. Tiemann, Phys. Rev. **130**, 617 (1963).

[9] H. Fritzsche and J. J. Tiemann, *Proceedings of the International Conference on the Physics of Semiconductors, Paris, 1964* (Academic Press Inc., New York, 1965), p. 599.